Materials Chemistry and Physics 158 (2015) 74–81

Contents lists available at ScienceDirect

Materials Chemistry and Physics

journal homepage: www.elsevier.com/locate/matchemphys

Comparison of tribological and electrochemical properties of TiN, CrN, TiAlN and a-C:H coatings in simulated body fluid

Qianzhi Wang [a, b, c], Fei Zhou [b, c], Chundong Wang [d], Muk-Fung Yuen [d], Meiling Wang [e], Tao Qian [f], Mitsuhiro Matsumoto [a], Jiwang Yan [a, *]

[a] Department of Mechanical Engineering, Faculty of Science and Technology, Keio University, Hiyoshi 3-14-1, Kohoku-ku, Yokohama, 223-8522, Japan
[b] State Key Laboratory of Mechanics and Control of Mechanical Structures, Nanjing University of Aeronautics and Astronautics, Nanjing, 210016, China
[c] College of Mechanical and Electrical Engineering, Nanjing University of Aeronautics and Astronautics, Nanjing, 210016, China
[d] Center of Super-Diamond and Advanced Films (COSDAF), Department of Physics & Materials Science, City University of Hong Kong, 83 Tat Chee Avenue, Kowloon, Hong Kong, China
[e] College of Materials Science and Technology, Nanjing University of Aeronautics and Astronautics, Nanjing, 210016, China
[f] StarArc Coating Technologies Co., Ltd., Suzhou, 215122, China

HIGHLIGHTS

- Hydration was a key factor to tribology of TiN, CrN and TiAlN coatings.
- CrN coating outperformed TiN, TiAlN and a-C:H coatings at tribology in SBF.
- CrN showed better corrosion resistance than those of TiN, TiAlN coatings in SBF.
- a-C:H coating presented the highest charge transfer resistance in SBF.
- The premature delamination of a-C:H coating occurred due to sensitivity to liquid.

GRAPHICAL ABSTRACT

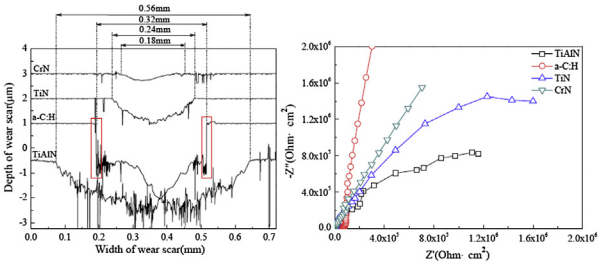

ARTICLE INFO

Article history:
Received 18 March 2014
Received in revised form
21 March 2015
Accepted 25 March 2015
Available online 29 March 2015

Keywords:
Thin films
Nitrides
Amorphous materials
Tribology
Electrochemical properties

ABSTRACT

TiN, CrN, TiAlN and a-C:H coatings have been used for wear reduction, but a thorough comparison of their erosion and abrasion characteristics in simulated body fluid (SBF) has never been reported in existent literature. In this study, the tribological and electrochemical performance of these coatings in SBF was investigated and compared. As a result, the TiAlN coating presented the worst tribological and electrochemical properties because of abundant products from hydration. On the contrary, due to the generation of a favorable tribochemical product (Cr_2O_3), the CrN coating exhibited superior characteristics of tribology and electrochemistry. The a-C:H coating also showed outstanding corrosion resistance, but premature delamination occurred in aqueous environment which might limit its application. Thus, the CrN coating was found to be the most favorable protection coating in SBF from a comprehensive viewpoint.

1. Introduction

Currently, cobalt–chromium alloy, titanium alloy and austenitic stainless steel are used as three major biomaterials to manufacture

* Corresponding author.
E-mail address: yan@mech.keio.ac.jp (J. Yan).

http://dx.doi.org/10.1016/j.matchemphys.2015.03.039
0254-0584/

Table 1
Electrochemical conditions and results in different Refs.

Coatings	Reference	Substrate	Solution	Temperature (°C)	E_{corr} (V)	I_{corr} (A/cm^2)
TiN	Pohrelyuk et al. [12]	Ti-6Al-4V	Ringer	36	−0.110	3.7×10^{-7}
	Jeon et al. [14]	316L	1 M H_2SO_4 and 2 ppm HF	70	0.038	2.3×10^{-7}
CrN	Chang et al. [18]	304	0.5 M H_2SO_4 and 1 M NaCl	25	–	4.0×10^{-7}
	William Grips et al. [19]	Mild steel	3.5% NaCl	25	−0.463	3.7×10^{-7}
TiAlN	William Grips et al. [19]	Mild steel	3.5% NaCl	25	−0.360	1.6×10^{-7}
	Li et al. [21]	$1Cr_{11}Ni_2W_2MoV$	0.5 mol/L NaCl	25	−0.378	1.7×10^{-7}
a-C:H	Hadinata et al. [22]	304 and 316L	3.5wt.% NaCl	25	–	2.0×10^{-8}
	Cai et al. [23]	NiTi alloy	Hank	37	−0.046	2.0×10^{-6}
	Azzi et al. [24]	316L	Ringer	25	–	1.0×10^{-11}

prosthesis replacements and fixation devices due to its excellent mechanical property, strong corrosion resistance and satisfactory biocompatibility in physiological environment [1–3]. Nevertheless, about 10% of hip arthroplasties need to be replaced after 10–15 years because of local corrosion and fretting fatigue, which result from the high Cl^- concentration and moderate temperature of human body fluid [4–11]. In order to prolong service life of prosthesis replacement, many kinds of corrosion-proof coatings have been introduced to enhance the surface electrochemical performance. These coatings can be divided into two major classes. One is transition metal nitride coatings, such as TiN [12–16], CrN [17–20] and TiAlN [19–21] while the other is amorphous carbon (a-C) coating [22–24]. Nevertheless, as shown in Table 1, the corrosion potential (E_{corr}) and corrosion current density (I_{corr}) of a-C:H, TiN, CrN and TiAlN coatings depend strongly on solutions, substrates and temperatures [12,14,18,19,21–24]. The I_{corr} of a-C:H coatings varies dramatically in a very broad range from 2.0×10^{-6} to 1.0×10^{-11} A/cm^2 under different electrochemical conditions. However, to date, there has been no available literature on the tribology of metal nitrides and amorphous carbon coatings in SBF. Moreover, the existing literature is concentrated on either tribology or electrochemistry, while studies on both tribology and electrochemistry of metal nitrides and amorphous carbon coating are very few [25], although in most application both the two kinds of properties are required simultaneously [26]. Thus, it is extremely important to clarify both the tribological and electrochemical performance of a-C:H, TiN, CrN and TiAlN coatings in SBF.

Among various transition metal nitride coatings, CrN coating is a paradox in biomedical applications because of the toxicity and advantage of Cr. The permissible amount of Cr for human body per day is about 1 mg. In this study, according to the wear rate of CrN coatings (8.81×10^{-7} mm^3/Nm), the release of Cr (7.15 g/cm^3) is around 0.01 mg under 2N (79 MPa) and 1000 m. Thus, this amount is affordable for humans because the pressure of a hip joint is much lower, around 1 MPa [27,28]. In addition, Cr is an essential trace element for humans because it helps us to absorb glucose.

In Refs. [29,30], a WC-Co interlayer was employed to enhance adhesion of coatings on steel substrate, and it was found that the interlayer also played a key role in determining friction behavior. For this reason, WC-Co interlayers are currently adopted when depositing coatings on biomaterials such as cobalt–chromium, titanium alloy and austenitic stainless. In this study, the structure of a WC-Co interlayer and a metal base was simplified by using cemented carbide (WC) as a substrate directly for depositing coatings.

In this study, the tribological and electrochemical properties of TiN, CrN, TiAlN and a-C:H coatings in SBF were evaluated by using a ball-on-disc tribometer and electrochemical impedance spectroscopy (EIS), respectively. Subsequently, the results of these four coatings were discussed from the viewpoint of tribochemistry.

2. Experimental details

2.1. Deposition and characterization of coatings

WC discs (8.0 at.% Co) with a dimension of Ø30 × 4 mm^3 and Si(100) wafers were used as substrates for tribotests and electrochemical tests, respectively. All of the coatings were fabricated by enhanced cathodic arc magnetron sputtering under electrical and magnetic fields simultaneously (Jupiter, StarArc Coating Technologies Co., Ltd., China), which could enhance ionization rate and improve the quality of coatings as a result. Prior to deposition, the substrates were ultrasonically cleaned in ethanol and deionized water in succession, and then further cleaned via Ar^+ bombardment for 10 min. During deposition process, the chamber pressure was remained at 0.8 Pa, and TiN, CrN, TiAlN and a-C:H coatings were synthesized by following procedures. Firstly, a Ti metal layer was deposited on the substrate in advance for all these coatings to increase the adhesive strength between the substrate and the top coating. Then a gradient TiN coating was synthesized via increasing the ratio of N_2 in mixed gases (Ar and N_2) from 10% to 100% while CrN and TiAlN coatings were deposited by sputtering Cr and TiAl metal targets, respectively. As for the a-C:H coating, after deposition of a Ti adhesive layer, the fabrication was conducted under the mixed atmosphere of Ar (10 sccm) and CH_4 (100 sccm) gases with constant ratio of 10%.

The crystal phases of TiN, CrN and TiAlN coatings were measured via D8-Advance X-ray diffraction (XRD) (Bruker, Germany) with Cu Kα radiation (λ = 0.15404 nm). A continuous scan mode was used to collect 2θ data from 10° to 100° at the sampling pitch of 0.02 and the scan rate of 2°/min. The X-ray tube voltage and current were set to 40 kV and 40 mA, respectively. Because of its

Table 2
Physical properties of TiAlN, a-C:H, TiN, CrN coatings and Al_2O_3 ball.

Materials	Thickness (μm)	Hardness (GPa)	Elastic modulus (GPa)	H^3/E^2	Average crystal size (nm)	Contact pressure (GPa)
TiAlN	1.89	27.3	466	0.094	32.4	0.706
a-C:H	1.79	16.7	166	0.169	–	0.479
TiN	0.76	23.6	397	0.083	33.2	0.673
CrN	2.05	17.9	422	0.032	37.9	0.685
Al_2O_3	–	16.5	370	0.032	–	–

Table 3
Chemical composition of simulated body fluid.

Compound	Concentration(g/L)
NaCl	7.996
$NaHCO_3$	0.35
KCl	0.22
$K_2HPO_4 \cdot 3H_2O$	0.228
$MgCl_2 \cdot 6H_2O$	0.305
$CaCl_2$	0.278
Na_2SO_4	0.071
$(CH_2OH)_3CNH_2$	6.057
1 mol/L HCl	For pH controlling

amorphous nature, the bonding condition of a-C:H coating was characterized by Raman spectroscopy (NRS-3100, JASCO Co. Ltd., Japan). In addition, the cross-section morphology and thickness of coatings were observed and measured via a field emission scanning electron microscope (FE-SEM) (JEOL-JSM-7001F). Regarding mechanical properties, the hardness and elastic modulus of coatings were measured via nanoindentation tester (ENT-1100a, Elionix Co. Ltd., Japan). The penetration depth of a Berkovich indenter was set to 100 nm, and 40 nanoindentations were performed under each condition. Table 2 lists the mechanical properties of TiN, CrN, TiAlN, a-C:H coatings and the Al_2O_3 ball.

2.2. Characterization of tribological properties

The friction behavior of coatings was investigated by a ball-on-disc tribometer, and the common material of articular head (Al_2O_3) was chosen as mating ball with a diameter of 8 mm. All the tribotests were carried out at 2 N, 0.2 m/s with a sliding distance of 1000 m. In this case, the friction coefficient of coatings/balls tribopair rather than that of WC/balls tribopair, as well as worn-out distance could be gained and compared at the same time. After friction test, the diameter of wear scar on ball was measured by an optical microscope (XJZ-6) whilst the cross-section area of the wear track on a coated disc was obtained via a non-contact white-light interferometer (CCI 3D, Taylor Hobson Ltd. UK).

2.3. Characterization of corrosion behavior

Prior to electrochemical test, a coated Si(100) wafer was firstly connected with a copper wire by conductive carbon tape, and then enveloped by 704 silicon rubber with 1 × 1 cm^2 exposing test area. Electrochemical measurement was performed by a standard three-electrode electrochemical cell which has been described in Ref. [26]. After immersion of specimen in electrolyte for 1 h, EIS was measured at open circuit potential (OCP) with an AC excitation of 10 mV over the frequency range from 1 mHz to 100 kHz. Each EIS measurement lasted for about 2.5 h, and was repeated three times

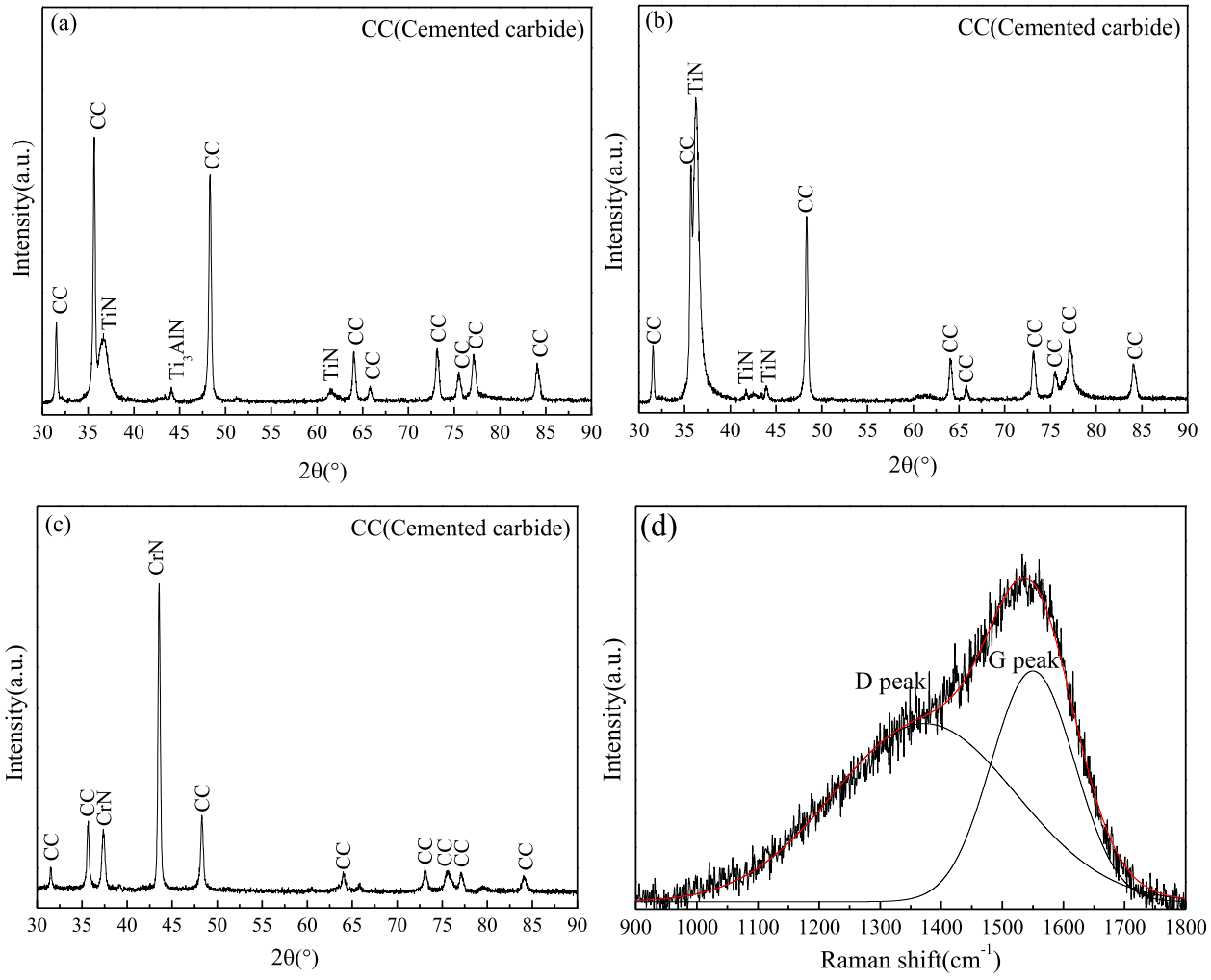

Fig. 1. X-ray diffraction spectra of (a) TiAlN, (b) TiN and, (c) CrN coatings and Raman spectrum of (d) a-C:H coating.

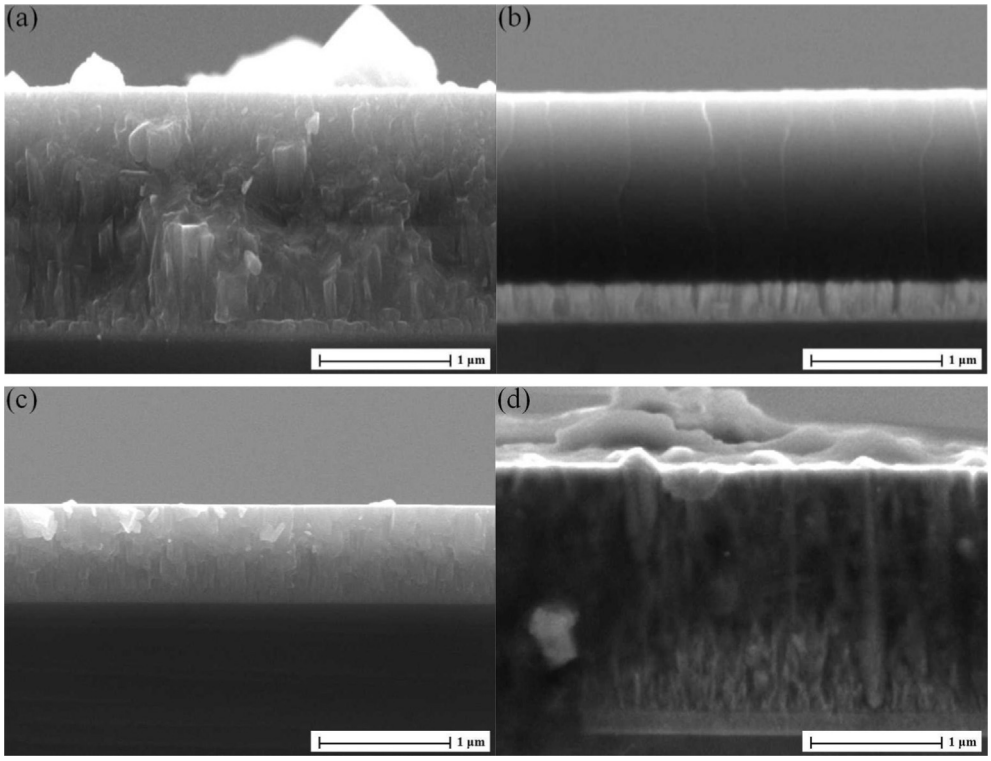

Fig. 2. Cross-sectional SEM images of (a) TiAlN, (b) a-C:H, (c) TiN and (d) CrN coatings.

by using new sample in fresh solution to ensure the reliability of data. Subsequently, the EIS data were fitted with equivalent circuit by ZsimpWin software.

All the above-mentioned measurements were carried out at 37 °C controlled by a water bath kettle (DF-101S), and simulated body fluid by formula (Table 3) was selected as lubricant for tribology and electrolyte for electrochemistry [31].

3. Results and discussion

3.1. Characterization of coatings

As seen in Fig. 1, except for the diffraction peaks of cemented carbides, TiAlN, TiN and CrN coatings all exhibit corresponding crystals of metal nitrides which sufficiently demonstrate the successful deposition. According to the Scherrer equation (1), the average crystal size (D) of each coating was calculated and is listed in Table 2.

$$D = K\lambda/B\cos\theta \quad (1)$$

where K is Scherrer constant of 0.89; λ is X-ray wavelength of

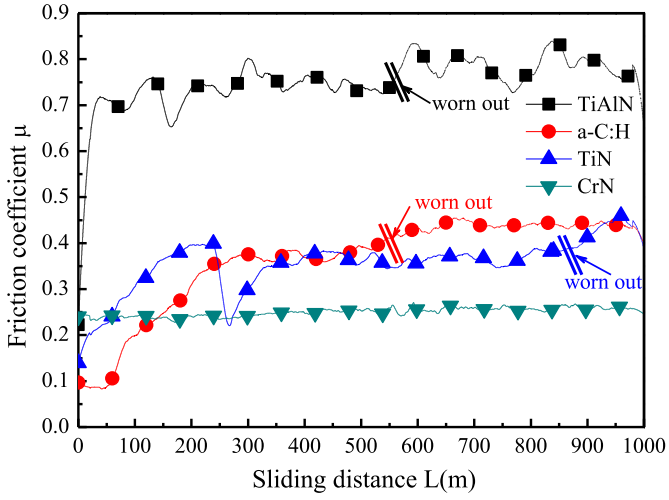

Fig. 3. The friction behavior of different coatings in SBF.

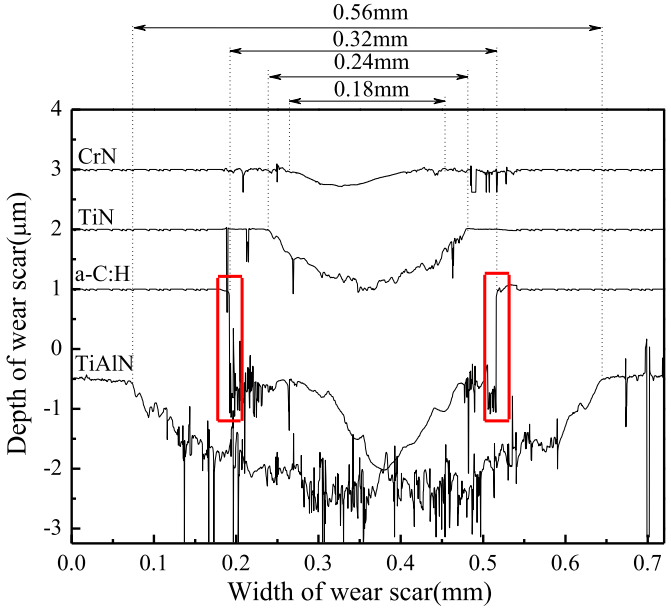

Fig. 4. The cross-sectional contour lines of wear tracks on different coatings.

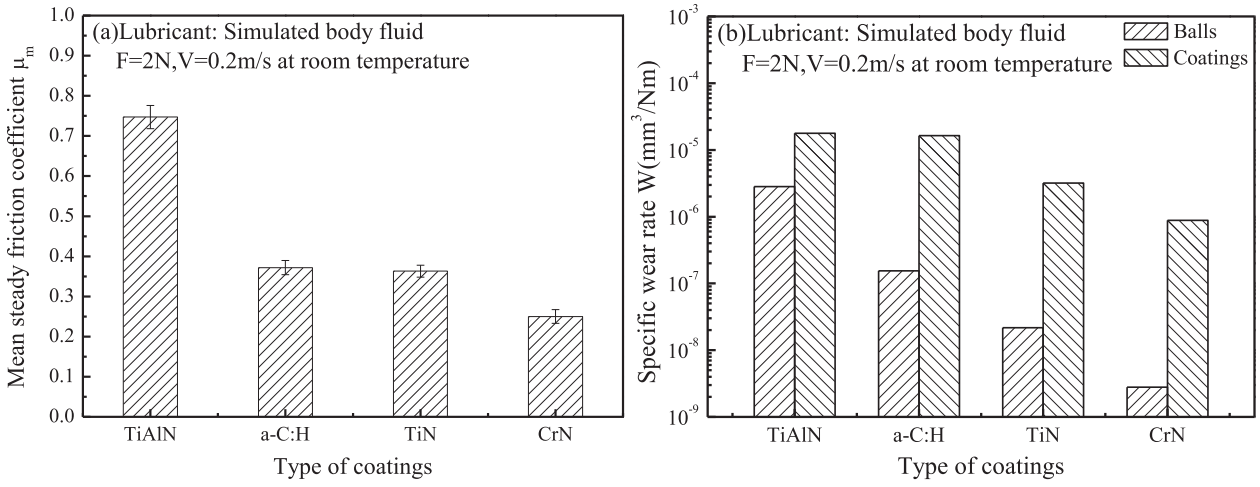

Fig. 5. The variation of (a) Mean steady friction coefficients and (b) Tribopairs' specific wear rates as a function of coatings' type.

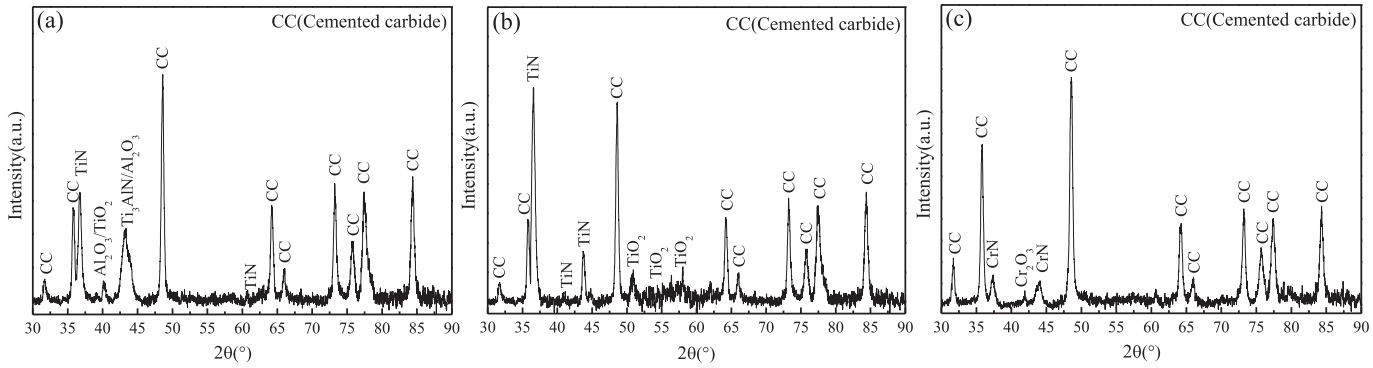

Fig. 6. X-ray diffraction spectra of wear tracks on (a) TiAlN (b) TiN and (c) CrN coatings.

0.15404 nm; B is Full-Width at Half Maximum (FWHM) and θ is diffraction angle. It is obvious that TiAlN coating presents a smaller average crystal size (32.4 nm) than TiN coating (33.2 nm) due to grain refinement by Al doping [32,33], while CrN coating shows the biggest average crystal size of 37.9 nm. As for the a-C:H coating, no specific crystal size is listed here due to amorphous nature characterized by Raman spectrum in Fig. 1d, in which obvious D (disordered carbon) and G (graphitic carbon) peaks appear simultaneously [34]. Accordingly, different average crystal sizes directly influence the compactness of these four coatings shown in Fig. 2. As compared with TiAlN and TiN coatings, the CrN coating displays columnar microstructure with greater cluster size while the a-C:H coating shows the most compact morphology due to its amorphous feature.

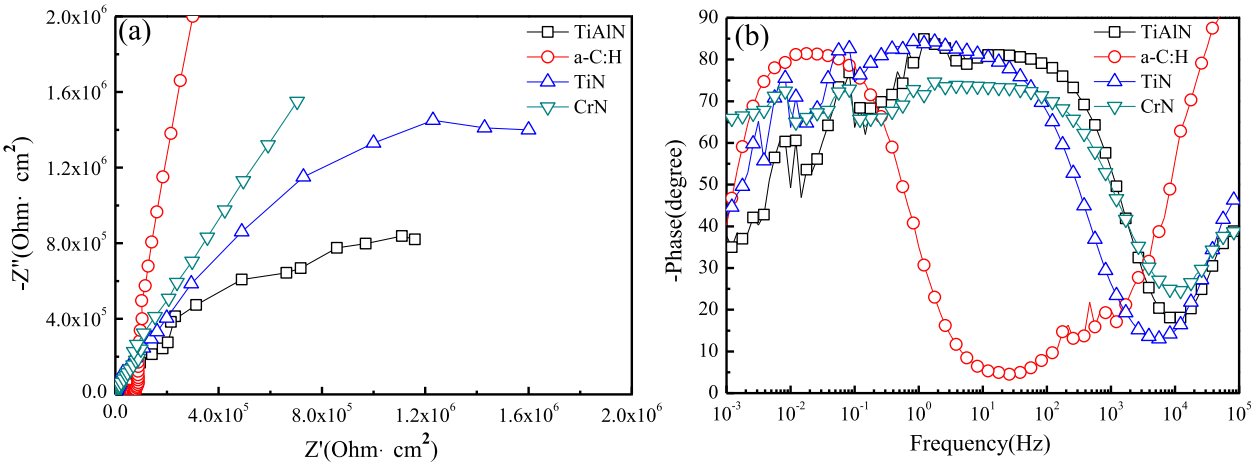

Fig. 7. (a) Nyquist plots (b) Bode plots of different coatings in SBF.

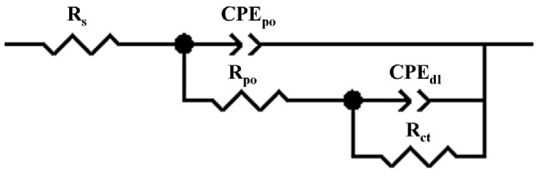

Fig. 8. Equivalent circuit of different coatings.

3.2. Tribological properties of coatings

According to Hertzian circular point contact, the initial contact pressures of different tribopairs were calculated (Table 2), and the order of contact pressure is TiAlN > CrN > TiN > a-C:H. For this reason, a similar variation trend of initial friction coefficient is shown among TiAlN (0.222), CrN (0.241), TiN (0.139) and a-C:H (0.097) coatings. On the other hand, the failure distance of each coating can be confirmed by sharp increase of friction coefficient in Fig. 3. It is clear that the TiAlN and a-C:H coatings were worn out at a distance of 550 m while the worn-out distance of TiN coating is 870 m. In contrast, the CrN coating remains its integrity, because its friction coefficient keeps stable during whole friction test. As seen in Fig. 4, the depths of wear tracks on the TiAlN, a-C:H and TiN coatings are 2.5 μm, 3 μm and 1 μm, which exceed the thicknesses of films (Table 2). Nevertheless, the depth of wear track on CrN coating is just 0.6 μm and lower than its thickness. Furthermore, the widths of wear tracks on these four coatings present similar variation trend as depths, and decrease from 0.56 mm (TiAlN) to 0.18 mm (CrN). Thus, taking the friction behavior (Fig. 3) and the contours (Fig. 4) into consideration, these two results are consistent with each other.

The mean-steady friction coefficients and specific wear rates of different tribopairs are illustrated in Fig. 5. Although TiAlN and a-C:H coatings exhibit relatively denser microstructure due to small crystal size and amorphous nature, TiN and CrN coatings outperform TiAlN and a-C:H coatings both at friction coefficient and wear rate. To be specific, TiN and CrN coatings exhibit lower friction coefficients (0.363 and 0.250, separately) and wear rates (3.19×10^{-6} mm^3/Nm and 8.81×10^{-7} mm^3/Nm, respectively) as compared with TiAlN and a-C:H coatings. Thus, average crystal size and compactness are not key factors to affect tribological properties. Generally, the resistance to plastic deformation of the coating is proportional to H^3/E^2 ratio, which reflects relative wear resistance to a certain extent. However, it is worth noting that the TiAlN and a-C:H coatings with higher H^3/E^2 ratios still present higher friction coefficients (0.747 and 0.372, respectively) and wear rates (1.78×10^{-5} mm^3/Nm and 1.64×10^{-5} mm^3/Nm, respectively). It is implied that hardness and elastic modulus are also irrelevant to tribological properties. Thus, there must be other factors contributing to this phenomenon. As compared with original XRD of coatings, some novel and weak peaks of oxides present in Fig. 6 after tribotest. According to our previous researches [35,36], the hydration of TiAlN, TiN and CrN coatings in aqueous environment can take place as reactions (2–4). Then, the corresponding oxides exhibit in individual XRD such as Al_2O_3/TiO_2 peak at 40.2° for TiAlN coatings, TiO_2 peaks at 50.8°, 56.3° and 58.1° for TiN coatings, and Cr_2O_3 peak at 41.5° for CrN coatings.

$$2TiAlN+7H_2O = 2TiO_2+Al_2O_3+2NH_3+4H_2 \quad (2)$$

$$\Delta G_f^{298} = -1370.58 \text{ kJ/mol}$$

$$2TiN + 4H_2O = 2TiO_2 + 2NH_3 + H_2 \quad (3)$$

$$\Delta G_f^{298} = -233.33 \text{ kJ/mol}$$

$$2CrN + 3H_2O = Cr_2O_3 + 2NH_3 \quad (4)$$

$$\Delta G_f^{298} = -250.10 \text{ kJ/mol}$$

Since the degree of reaction is proportional to Gibbs free energy, the hydration of TiAlN coating occurs much easier than those of TiN and CrN coatings. Therefore, significant products originate from the chemical reaction (2), and compels TiAlN coating to suffer higher specific wear rate as compared with TiN and CrN coatings. On basis of this, extremely rough contact area is formed by severe wear, and subsequently $TiAlN/Al_2O_3$ tribopair exhibits the highest friction coefficient of 0.747. As for a-C:H coating, the hydrogen originating from CH_4 makes it be sensitive to aqueous environment, and causes delamination easily [37,38]. As seen in Fig. 4, it is worth noting that the edge of wear track in red frame is quite different from the others, i.e., the edge is very neat. Thus, this phenomenon might be attributed to entire delamination under contact stress, and therefore, a-C:H coating presents high wear rate of 1.64×10^{-5} mm^3/Nm. However, during tribotest, falling a-C:H coating can stay between the contact surfaces, and offers self-lubrication effect indicated as a relatively low friction coefficient of 0.372. According to respective Gibbs free energy, the hydration degree of TiN and CrN coatings is quite similar, and therefore, the qualities of TiO_2 and Cr_2O_3 dominate the difference in tribology. Ozturk et al. [39] pointed out that the high friction of TiN coating was attributed to the formation of TiO_x while the relatively low friction of CrN coating was attributed to the oxygen-rich tribofilms. The oxide of Cr is of lower shear strength as compared with TiO_x. Thus, CrN coating exhibits a smoother wear track than that of TiN coating in Fig. 4, and reveals the lowest friction coefficient and specific wear rate.

3.3. Electrochemical properties of coatings

As seen in Fig. 7a, a-C:H coating exhibits the largest capacitive resistance arc followed by CrN coating, whereas TiAlN coating shows the smallest one. It is indicated that a-C:H coating can present better corrosion-proof ability as compared with other coatings in SBF. However, the phase of a-C:H coating at medium frequency (10^0–10^3 Hz) is lower than 30° in Bode plots (Fig. 7b). In contrast, CrN coating exhibits higher phase than 65° over a very broad frequency range from 10^{-3}–10^2 Hz. It is indicated that CrN coating would be more likely to perform as ideal capacitor during a broader

Table 4
Characteristics of the equivalent circuit derived from the EIS data in SBF.

Coatings	R_s(Ohm cm^2)	$(CPE\text{-}Y_o)_{po}$ (F cm^{-2})	$(CPE\text{-}n)_{po}$	R_{po} (ohm cm^2)	$(CPE\text{-}Y_o)_{dl}$ (F cm^{-2})	$(CPE\text{-}n)_{dl}$	R_{ct} (ohm cm^2)
TiAlN	1.93	8.85×10^{-6}	0.733	9.71	1.23×10^{-5}	0.998	2.23×10^6
a-C:H	0.89	4.36×10^{-10}	0.998	6.81×10^4	3.07×10^{-6}	0.926	4.70×10^7
TiN	1.23	3.26×10^{-6}	0.790	16.36	3.01×10^{-5}	0.984	2.92×10^6
CrN	2.47	1.42×10^{-5}	0.705	13.61	2.18×10^{-5}	0.883	2.15×10^7

frequency range, and prevents from electrolyte attacking.

According to Nyquist, Bode plots and chi-square values after ZsimpWin software fitting, the EIS data of all coatings can be well depicted by equivalent circuit with two time constants in Fig. 8, which has been used frequently to describe the AC response of a defective film on a metallic substrate [40]. In the equivalent circuit (EC), the electrolyte resistance R_s, originates from the ohmic contribution of the electrolyte solution between the working and reference electrodes; the pore resistance R_{po} related to the coatings' block effect will hinder the electrolyte penetration, and the CPE_{po} is the corresponding coatings' capacitance; the R_{ct} is related to charge transfer resistance due to the formation of a double layer of charge at the Si/electrolyte interface, and CPE_{dl} is the corresponding double-layer capacitance. Moreover, constant phase element (CPE or Q) is used to represent a non-ideal capacitor, and also to describe the deviation from the actual capacitive behavior [41]. The impedance of Q (Z_Q) is expressed as:

$$Z_Q = 1/[Y_o(j\omega)^n]. \quad (5)$$

where Y_o is the capacitance ($F\,cm^{-2}$), ω is the angular frequency (rd/s), j is $\sqrt{-1}$ and n is the CPE power that represents the degree of deviation from a pure capacitor. For $n = 1$, Q is an ideal capacitor, while for $n < 1$, Q is non-ideal.

The respective value of each component is listed in Table 4. Owing to the compact structure originating from amorphous nature, electrolyte is not easy to penetrate through a-C:H coating, and a-C:H coating shows the highest R_{ct} of $4.70 \times 10^7\ \Omega\ cm^2$. As we said in introduction, Cr is a paradox in biomedical application, but it still makes CrN coating present a slightly lower R_{ct} of $2.15 \times 10^7\ \Omega\ cm^2$. Without chromium, corrosion resistance of TiN and TiAlN coating becomes worse, especially for TiAlN coating, which exhibits the lowest value of $2.23 \times 10^6\ \Omega\ cm^2$. Since tribological tests were also conducted in SBF, the electrochemical properties of coatings definitely make an indirect influence on their tribological properties. Thus, CrN coating with relatively higher R_{ct} exhibits favorable tribological property, whereas TiAlN coating exhibits both the worst tribological and electrochemical properties. As for a-C:H coating, early delamination limits its applications in SBF even with the best corrosion resistance. In consequence, taking tribological and electrochemical properties into account, CrN coating is the favorable candidate which can be used in surgical prosthesis replacement.

4. Conclusion

The tribological and electrochemical properties of TiN, CrN, TiAlN and a-C:H coatings in SBF were investigated, and conclusions are drawn as follows:

(1) A CrN coating exhibits superior friction and wear ability due to tribochemical reaction, and presents better corrosion resistance in SBF than those of TiAlN and TiN coatings.
(2) In contrast, a TiAlN coating presents the worst tribological and electrochemical properties due to significant generation of wear debris from hydration.
(3) Although an a-C:H coating exhibits the highest R_{ct}, early delamination resulting from sensitivity to aqueous environment limits its application in SBF.

Acknowledgment

This work was supported by National Natural Science Foundation of China (Grant No. 51375231), the Research Fund for the Doctoral Program of Higher Education (Grant No. 20133218110030), and a grant for joint research in Keio University.

References

[1] S.M. Hosseinalipour, A. Ershad-langroudi, A.N. Hayati, A.M. Nabizade-Haghighi, Characterization of sol-gel coated 316L stainless steel for biomedical applications, Prog. Org. Coat. 67 (2010) 371–374.
[2] J. Pellier, J. Geringer, B. Forest, Fretting-corrosion between 316L SS and PMMA: influence of ionic strength, protein and electrochemical conditions on materialwear. Application to orthopaedic implants, Wear 271 (2011) 1563–1571.
[3] F. Yildiz, A.F. Yetim, A. Alsaran, A. Celik, I. Kaymaz, Fretting fatigue properties of plasma nitrided AISI 316L stainless steel: experiments and finite element analysis, Tribol. Int. 44 (2011) 1979–1986.
[4] K. Nielsen, Corrosion of metallic implants, Br. Corros. J. 22 (1987) 272–278.
[5] S.A. Brown, K. Merritt, Fretting corrosion in saline and serum, J. Biomed. Mater. Res. 15 (1981) 479–488.
[6] H. Placko, S. Brown, J. Payer, Release of cobalt and nickel from a new total finger joint prosthesis made of vitallium, J. Biomed. Mater. Res. 17 (1983) 655–668.
[7] V. Singh, K. Marchev, C.V. Cooper, E.I. Meletis, Intensified plasma-assisted nitriding of AISI 316L stainless steel, Surf. Coat. Technol. 160 (2002) 249–258.
[8] S. Carmignato, M. Spinelli, S. Affatato, E. Savio, Uncertainty evaluation of volumetric wear assessment from coordinate measurements of ceramic hip joint prostheses, Wear 270 (2011) 584–590.
[9] J. Geringer, W. Tatkiewicz, G. Rouchouse, Wear behavior of PAEK, poly(aryl-ether-ketone), under physiological conditions, outlooks for performing these materials in the field of hip prosthesis, Wear 271 (2011) 2793–2803.
[10] R. Crowninshield, A. Rosemberg, S. Sporer, Changing demographics of patients with total joint replacement, Clin. Orthop. Relat. Res. 443 (2006) 266–272.
[11] D.F.G. Emery, H.J. Clarke, M.L. Grover, Stanmore total hip replacement in younger patients: review of a group of patients under 50 years of age, J. Bone Jt. Surg. 79 (1997) 240–246.
[12] I.M. Pohrelyuk, V.M. Fedirko, O.V. Tkachuk, R.V. Proskurnyak, Corrosion resistance of Ti-6Al-4V alloy with nitride coatings in Ringer's solution, Corros. Sci. 66 (2013) 392–398.
[13] Z. Liu, D.R. Yan, Y.C. Dong, Y. Yang, Z.H. Chu, Z. Zhang, The effect of modified epoxy sealing on the electrochemical corrosion behaviour of reactive plasma-sprayed TiN coatings, Corros. Sci. 75 (2013) 220–227.
[14] W.S. Jeon, J.G. Kim, Y.J. Kim, J.G. Han, Electrochemical properties of TiN coatings on 316L stainless steel separator for polymer electrolyte membrane fuel cell, Thin Solid Films 516 (2008) 3669–3672.
[15] N.D. Nam, J.G. Kim, W.S. Hwang, Effect of bias voltage on the electrochemical properties of TiN coating for polymer electrolyte membrane fuel cell, Thin Solid Films 517 (2009) 4772–4776.
[16] X.B. Zhao, D.R. Yan, S. Li, C.G. Lu, The effect of heat treatment on the electrochemical corrosion behavior of reactive plasma-sprayed TiN coatings, Appl. Surf. Sci. 257 (2011) 10078–10083.
[17] A.B. Cristobal, A. Conde, J. Housden, T.J. Tate, R. Rodriguez, F. Montala, J. de Damborenea, Electrochemical stripping of hard ceramic chromium nitride coatings, Thin Solid Films 484 (2005) 238–244.
[18] K.L. Chang, S.C. Chung, S.H. Lai, H.C. Shih, The electrochemical behavior of thermally oxidized CrN coatings deposited on steel by cathodic arc plasma deposition, Appl. Surf. Sci. 236 (2004) 406–415.
[19] V.K. William Grips, V. Ezhil Selvi, Harish C. Barshilia, K.S. Rajam, Effect of electroless nickel interlayer on the electrochemical behavior of single layer CrN, TiN, TiAlN coatings and nanolayered TiAlN/CrN multilayer coatings prepared by reactive dc magnetron sputtering, Electrochim. Acta 51 (2006) 3461–3468.
[20] V.K. William Grips, Harish C. Barshilia, V. Ezhil Selvi, Kalavati, K.S. Rajam, Electrochemical behavior of single layer CrN, TiN, TiAlN coatings and nanolayered TiAlN/CrN multilayer coatings prepared by reactive direct current magnetron sputtering, Thin Solid Films 514 (2006) 204–211.
[21] Y. Li, L. Qu, F.H. Wang, The electrochemical corrosion behavior of TiN and (Ti,Al)N coatings in acid and salt solution, Corros. Sci. 45 (2003) 1367–1381.
[22] S.S. Hadinata, M.T. Lee, S.J. Pan, W.T. Tsai, C.Y. Tai, C.F. Shih, Electrochemical performances of diamond-like carbon coatings on carbon steel, stainless steel, and brass, Thin Solid Films 529 (2013) 412–416.
[23] W. Cai, J.H. Sui, Effect of working pressure on the structure and the electrochemical corrosion behavior of diamond-like carbon (DLC) coatings on the NiTi alloys, Surf. Coat. Technol. 201 (2007) 5194–5197.
[24] M. Azzi, P. Amirault, M. Paquette, J.E. Klemberg-Sapieha, L. Martinu, Corrosion performance and mechanical stability of 316L/DLC coating system: role of interlayers, Surf. Coat. Technol. 204 (2010) 3986–3994.
[25] L. Wang, J.F. Su, X. Nie, Corrosion and tribological properties and impact fatigue behaviors of TiN- and DLC-coated stainless steels in a simulated body fluid environment, Surf. Coat. Technol. 205 (2010) 1599–1605.
[26] Q.Z. Wang, F. Zhou, Z.F. Zhou, C.D. Wang, W.J. Zhang, L.K.-Y. Li, S.-T. Lee, Effect of titanium or chromium content on the electrochemical properties of amorphous carbon coatings in simulated body fluid, Electrochim. Acta 112 (2013) 603–611.
[27] F. Liu, J. Fisher, Z.M. Jin, Effect of motion inputs on the wear prediction of artificial hip joints, Tribol. Int. 63 (2013) 105–114.
[28] M.S. Uddin, L.C. Zhang, Predicting the wear of hard-on-hard hip joint prostheses, Wear 301 (2013) 192–200.

[29] G. Bolelli, L. Lusvarghi, M. Montecchi, F. Pighetti Mantini, F. Pitacco, H. Volz, M. Barletta, HVOF-sprayed WC-Co as hard interlayer for DLC films, Surf. Coat. Technol. 203 (2008) 699–703.
[30] Q.P. Wei, Z.M. Yu, M.N.R. Ashfold, L. Ma, Z. Chen, Fretting wear and electrochemical corrosion of well-adhered CVD diamond films deposited on steel substrates with a WC-Co interlayer, Diam. Relat. Mater. 19 (2010) 1144–1152.
[31] P.J. Li, C. Ohtsuki, T. Kokubo, K. Nakanishi, N. Soga, Apatite formation induced by silica gel in a simulated body fluid, J. Am. Ceram. Soc. 75 (1992) 2094–2097.
[32] S.Y. Yoon, J.K. Kim, K.H. Kim, A comparative study on tribological behavior of TiN and TiAlN coatings prepared by arc ion plating technique, Surf. Coat. Technol. 161 (2002) 237–242.
[33] G.T. Liu, J.G. Duh, K.H. Chung, J.H. Wang, Mechanical characteristics and corrosion behavior of (Ti,Al)N coatings on dental alloys, Surf. Coat. Technol. 200 (2005) 2100–2105.
[34] C. Casiraghi, A.C. Ferrari, J. Robertson, Raman spectroscopy of hydrogenated amorphous carbons, Phys. Rev. B Condens. Matter 72 (085401) (2005) 1.
[35] Q.Z. Wang, F. Zhou, X.N. Wang, K.M. Chen, M.L. Wang, T. Qian, Y.X. Li, Comparison of tribological properties of CrN, TiCN and TiAlN coatings sliding against SiC balls in water, Appl. Surf. Sci. 257 (2011) 7813–7820.
[36] F. Zhou, K.M. Chen, M.L. Wang, X.J. Xu, H. Meng, M. Yu, Z.D. Dai, Friction and wear properties of CrN coatings sliding against Si_3N_4 balls in water and air, Wear 265 (2008) 1029–1037.
[37] H. Ronkainen, S. Varjus, K. Holmberg, Friction and wear properties in dry, water- and oil-lubricated DLC against alumina and DLC against steel contacts, Wear 222 (1998) 120–128.
[38] H. Ronkainen, S. Varjus, K. Holmberg, Tribological performance of different DLC coatings in water-lubricated conditions, Wear 249 (2001) 267–271.
[39] A. Ozturk, K.V. Ezirmik, K. Kazmanli, M. Urgen, O.L. Eryılmaz, A. Erdemir, Comparative tribological behaviors of TiN–, CrN– and MoN–Cu nanocomposite coatings, Tribol. Int. 41 (2008) 49–59.
[40] F. Mansfeld, Use of electrochemical impedance spectroscopy for the study of corrosion protection by polymer coatings, J. Appl. Electrochem. 25 (1995) 187–202.
[41] C. Liu, Q. Bi, A. Leyland, A. Mattews, An electrochemical impedance spectroscopy study of the corrosion behaviour of PVD coated steels in 0.5 N NaCl aqueous solution: part I. Establishment of equivalent circuits for EIS data modelling, Corros. Sci. 45 (2003) 1243–1256.